Geol. Mag. **140** (*3*), *2003, pp. 343–355. © 2003 Cambridge University Press*
DOI: 10.1017/S001675680300757X *Printed in the United Kingdom*

Palaeomagnetic evolution of the Çankırı Basin (central Anatolia, Turkey): implications for oroclinal bending due to indentation

NURETDIN KAYMAKCI*, CHARON E. DUERMEIJER†, COR LANGEREIS†, STANLEY H. WHITE† & PAUL M. VAN DIJK‡

*Middle East Technical University, Faculty of Engineering, Dept. of Geological Engineering, 06531-Ankara, Turkey
†Faculty of Earth Sciences, Utrecht University, Budapestlaan 17, 3584 CD Utrecht, The Netherlands
‡ITC, Hengelosestr 99, P.O. Box 6, 7500 AA Enschede, The Netherlands

(*Received* 7 May 2002; *accepted* 12 November 2002)

Abstract – Palaeomagnetic data in combination with palaeostress data and anisotropy of magnetic susceptibility orientations are utilized to develop a tectonic evolutionary model for the Early Tertiary part of the Ω (omega)-shaped Çankırı Basin (Turkey). The results reveal clockwise rotations in the northeast and anticlockwise rotations in the west and southeastern corner of the basin. The magnetic inclinations indicate a northward drift of the Çankırı Basin and support an indentation model for the Kırşehir Block. It is proposed that the Ω-shape of the Çankırı Basin was the result of indentation of the Kırşehir Block into the Sakarya Continent during northwards migration accompanying closure of Neotethys. It appears that the indentation started prior to Eocene and ended before Middle Miocene times.

Keywords: tectonics, palaeomagnetism, magnetic declination, stress, Turkey, oroclines.

1. Introduction

The pre-Neogene tectonic history of Turkey is mainly dominated by the amalgamation of a number of tectonic blocks (micro-continents) which were once part of Laurasia and Gondwana (Şengör & Yılmaz, 1981; Görür *et al*. 1984; Robertson & Dixon, 1984; Şengör, Yılmaz & Sungurlu, 1984; Dercourt *et al*. 1993; Channell *et al*. 1996; Robertson *et al*. 1996). Turkey is broadly divided into three tectonic belts. These are (Fig. 1a), from north to south, the Pontides, Anatolides and the Taurides (Ketin, 1966). The Pontides are the eastern continuation of the Rhodope–Pontide fragments including the Sakarya Continent (Şengör & Yılmaz, 1981; Şengör, Yılmaz & Sungurlu, 1984). The Anatolides are the metamorphic northern continuation of the Taurides (Şengör & Yılmaz, 1981) and include the Menderes Massif and the Kırşehir Block. The Sakarya Continent and the Kırşehir Block each had a different geological evolution from Late Palaeozoic to Mesozoic times (Şengör & Yılmaz, 1981; Şengör, Yılmaz & Sungurlu, 1984). The Sakarya Continent was separated from the rest of the Pontides by the Intra-Pontide Ocean during Early Mesozoic times (Robertson & Dixon, 1984; Şengör, Yılmaz & Sungurlu, 1984; Tüysüz, 1993), while the Kırşehir Block was separated from the Taurides by the Intra-Tauride ocean (Görür *et al*. 1984). However, the Kırşehir Block has the same stratigraphic characteristics as the Taurides, which has experienced a similar evolutionary history. Further, it has been proposed (Şengör & Yılmaz, 1981; Görür *et al*. 1984; Şengör, Yılmaz & Sungurlu, 1984) that the two micro-continents, namely the Sakarya Continent and Kırşehir Block, were separated from each other by the main branch of the Tethys Ocean throughout the Mesozoic and both drifted from equatorial latitudes in Late Cretaceous times to their present positions (Şengör, Yılmaz & Sungurlu, 1984; Robertson *et al*. 1996). Although the timing of collision and amalgamation of these two micro-continents along the Izmir–Ankara–Erzincan Suture Zone (IAESZ, see Fig. 1) is debated, it is generally constrained within the Late Cretaceous to Early Tertiary interval (Şengör & Yılmaz, 1981; Görür *et al*. 1984; Tüysüz, 1993; Koçyiğit, Özkan & Rojay, 1988; Koçyiğit, 1991; Okay, Harris & Kelley, 1998). According to Sanver & Ponat (1981) and Görür *et al*. (1984), the Kırşehir Block has rotated 104° anticlockwise and drifted northwards since Cretaceous times.

Furthermore, the Late Miocene collision and further convergence of the Arabian Block in the south, and the Eurasian Plate in the north, along the Bitlis–Zagros Suture (BZS), resulted in the westward expulsion of the Anatolian Block (Fig. 1b) along the North Anatolian (NAFZ) and East Anatolian transform fault zones (EAFZ) (Şengör & Yılmaz, 1981; Şengör, Şaroğlu & Görür, 1985). The Anatolian Block continues to deform internally, which is characterized by dominant regional transcurrent deformation in the east and a dominant extensional deformation in the west (Şengör, Şaroğlu & Görür, 1985). In the north central part of

* Author for correspondence: nkaymakci@yahoo.com

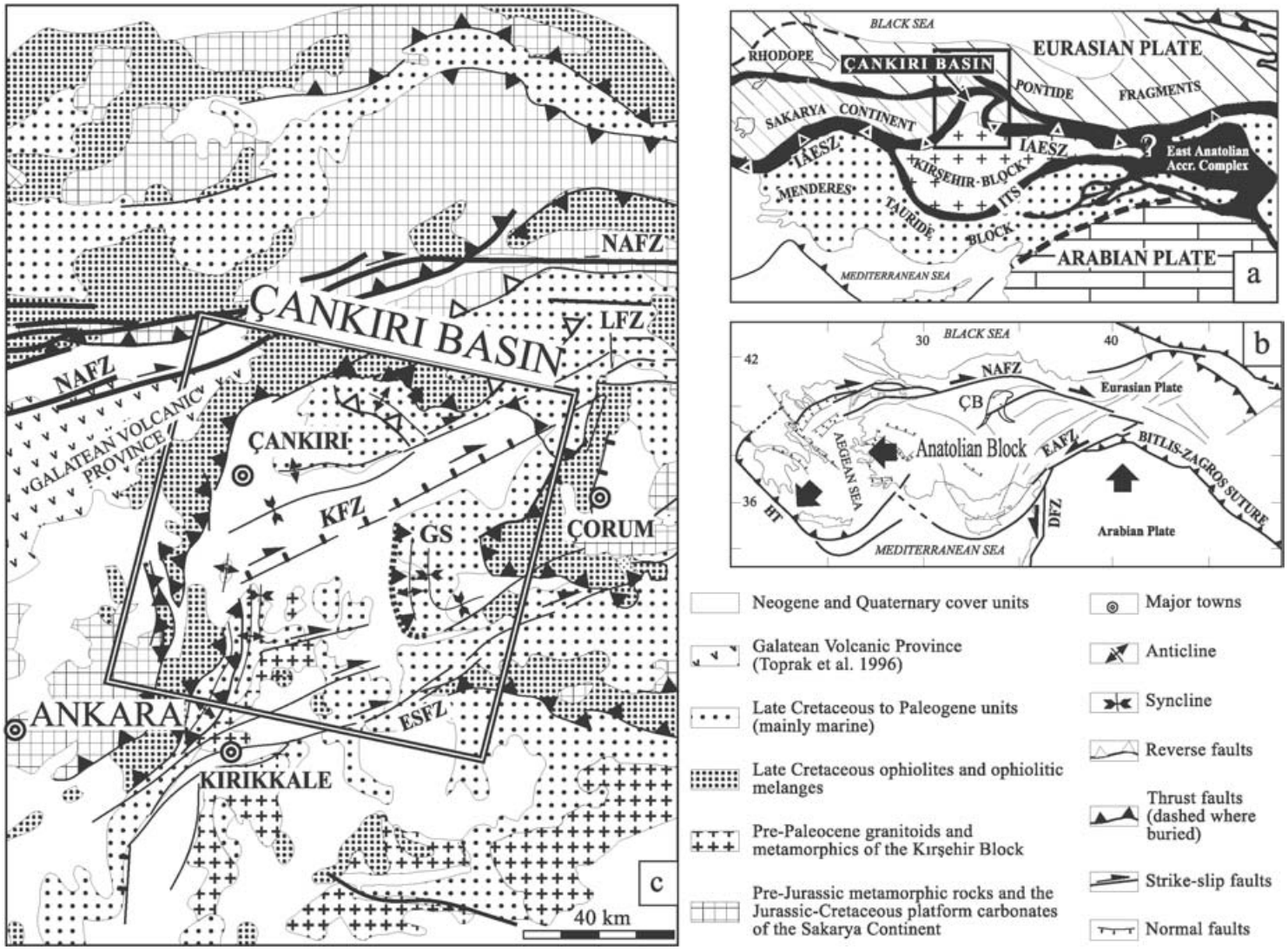

Figure 1. (a) Inset map showing the geological outline of Eastern Mediterranean area (Modified after Şengör, Yılmaz & Sungurlu, 1984). IAESZ – Izmir–Ankara–Erzincan Suture Zone; ITS – Inner-Tauride Suture. (b) Tectonic setting of the Eastern Mediterranean area. Thick lines are major strike-slip faults, thinner lines are second order strike-slip faults. Large black arrows indicate plate movement directions. ÇB – Çankırı Basin; DFZ – Dead Sea Fault zone; EAFZ – East Anatolian Fault Zone; HT – Hellenic Trench; NAFZ – North Anatolian Fault Zone (modified after Barka & Hancock, 1984; Kaymakci & Koçyiğit, 1995). (c) Tectono-stratigraphic map of central Anatolia. Box shows the location of the Çankırı Basin. Note Ω-shape of outline of the ophiolitic rim of the Çankırı Basin. ESFZ – Ezinepazarı–Sungurlu Fault Zone; GS – Güvendik Syncline; KFZ – Kızılırmak Fault Zone; LFZ – Laçin Fault Zone; NAFZ – North Anatolian Fault Zone.

the Anatolian Block, a number of northwards convex dextral strike-slip faults divide the region into roughly E–W-oriented wedges (Fig. 1b) that branch off from the North Anatolian Fault Zone (Barka & Hancock, 1984; Kaymakci & Koçyiğit, 1995; Barka, 1992). Deformation of these wedges is marked by a complex rotational strain (Kaymakci & Koçyiğit, 1995; Piper *et al*. 1996; Oral *et al*. 1997).

Previous palaeomagnetic studies in Turkey have mainly dealt with the determination of palaeolatitudes of the amalgamated micro-continents and of their apparent polar wander path (e.g. Van der Voo, 1968; Sanver & Ponat, 1981; Evans & Hall, 1990; Morris & Robertson, 1993; Channell *et al*. 1996) and indicate a northwards drift of the tectonic blocks south of the Pontides (including the Sakarya Continent and the Kırşehir Block), from equatorial latitudes in the Late Cretaceous to their present positions. Other studies have concentrated on block rotations along the North Anatolian Fault Zone and within the Anatolian Block (e.g. Saribudak *et al*. 1990; Platzman *et al*. 1994; Platzman, Tapirdamaz & Sanver, 1998; Michel *et al*. 1995; Tatar *et al*. 1995; Piper *et al*. 1996; Piper, Tatar & Gürsoy, 1997; Gürsoy *et al*. 1997). The detected post-Late Miocene dominantly anticlockwise rotations are generally in agreement with the Geographic Positioning System (GPS) measurements (Oral *et al*. 1997).

The Çankırı Basin straddles the Pontides in the north and the Kırşehir Block in the south (Fig. 1). It lies above the Izmir–Ankara–Erzincan Suture Zone (IAESZ), which has an overall E–W trend but to the east of Ankara, this suture zone makes a sharp bend in an Ω−shape around the basin. In its western, northern and eastern rim, the Çankırı Basin is surrounded by the North Anatolian Ophiolitic Melange (NAOM, terminology after B. F. Rojay, unpub. Ph.D. thesis, METU, 1993; Rojay, 1995) and associated Late Cretaceous units (Fig. 2). In the south it is delimited by granitoids of the Kırşehir Block. It has evolved from Late Cretaceous to Early Miocene times due to collision and indentation of the Sakarya Continent and the Kırşehir Block (Kaymakci, 2000). Late Cretaceous to Recent continuous infill (Fig. 2) makes it one of the best test sites in north central Turkey, which may provide sufficient magnetic information to understand the rotation of the suture zone and the basin infill. Therefore, this study aims to understand the mechanism and

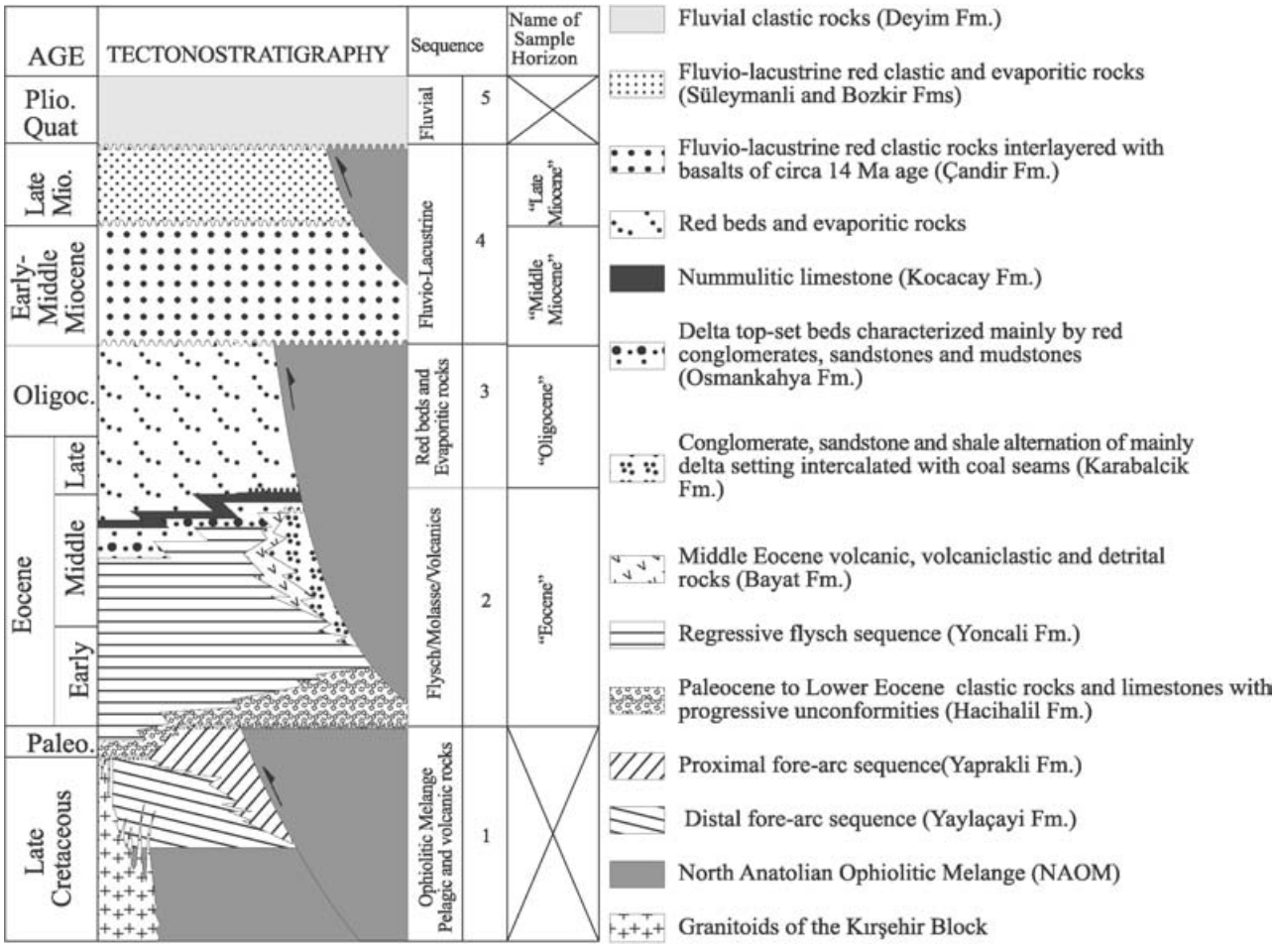

Figure 2. Simplified tectono-stratigraphic column of the units exposed in the Çankırı Basin (see Kaymakci, 2000).

timing of rotational processes which resulted in the Ω−shape of the Çankırı Basin (Kaymakci, 2000) using palaeomagnetic analysis and to discuss the kinematics of rotation processes using palaeostress data published elsewhere (Kaymakci, 2000; Kaymakci, White & Van Dijk, 2000). Furthermore, this study intends to shed some light on the palaeomagnetic characteristics of the region and provide constraints on the subduction history of the Tethys and collisional processes that took place in Late Cretaceous to Early Miocene times.

2. Geological setting of the Çankırı Basin

The Çankırı Basin comprises more than 4 km thick sedimentary infill ranging from Late Cretaceous to Recent in age and which accumulated in five sequences of sedimentation (A. A. Dellaloğlu *et al*., unpub. report, 1992; see also Kaymakci, 2000; summarized in Fig. 2).

The oldest sedimentary sequence consists of tectonically intercalated Late Cretaceous deep marine sediments alternating with mafic volcanic rocks, volcanoclastic rocks, proximal regressive shallow marine units and Paleocene littoral red clastic rocks and carbonates, which represent the subduction history of the northern Neotethys in the region (Koçyiğit, 1991; Y. Özçelik, unpub. M.Sc. thesis, METU, 1994; Tüysüz, Dellaloğlu & Terzioğlu, 1995). The second sequence is a Late Paleocene to mid-Oligocene, more than 1 km thick, regressive flysch to molasse type succession intercalated with mafic to intermediate volcanic rocks and a nummulitic limestone. The third sequence comprises a very thick (up to 2 km) sequence of Late Eocene to mid-Oligocene continental red clastic rocks and evaporites. The fourth sequence is up to 1 km thick and represented by Early Miocene to Pliocene fluvio-lacustrine deposits. The Late Pliocene–Quaternary alluvial fan deposits and recent alluvium locally overlie all these units (Fig. 2; see Kaymakci, 2000)

The main structures shaping the current geometry of the Çankırı Basin (Fig. 1) are the thrust and reverse faults delineating the western and northern rims of the Çankırı Basin. The eastern margin is defined by a belt of NNE-striking folds. In the south, the basin infill onlaps the basement (Kırşehir Block) (Kaymakci, 2000). The thrust and reverse faults noted above developed in Late Cretaceous to Early Tertiary times during subduction and the subsequent collision of the Kırşehir Block and the Sakarya Continent and were reactivated during the post-Middle Miocene evolution of the basin (Kaymakci, White & Van Dijk, 1998, 2000; see also Kaymakci, 2000). The other major structures affecting the Çankırı Basin are the Kızılırmak Fault zone (KFZ) and Ezinepazarı–Sungurlu Fault zone (ESFZ) which are oriented WSW–ENE and have dextral strike-slip character. They displace the ophiolitic rim, the basement and the basin infill including the Late Miocene units and indicate a post-Late Miocene tectonic activity (Kaymakci, White & Van Dijk, 2003).

3. Palaeomagnetic results

Sampling was performed on the second, third and fourth sequences of the basin infill (Fig. 2), namely the Early to Middle Eocene (sequence 2), the Late Eocene to Oligocene (sequence 3), the Middle Miocene (lower part of the sequence 4), and the Late Miocene (upper part of sequence 4). The ages of the studied units of sequence 2 are based on marine fauna (see Kaymakci, 2000). The age of sequence 3 is based on superposition, due to lack of fossil evidence, and partly on micromammals obtained only in two localities in the upper part of the sequence as is sequence 4. Throughout this text sequence 2 is referred to as 'Eocene' and sequence 3 as 'Oligocene'.

In all sites, sampling was performed using an electrical drill and a portable generator. Care was taken to avoid sampling near large faults. After removing the weathered surface to reach fresh clays, we took at least seven standard oriented palaeomagnetic cores at each site. Mostly fine-grained sediments were sampled which are generally deposited with a low sedimentation rate. Sampling over a sufficiently large interval tends to average out secular variations in these rocks. In addition, early post-depositional processes typically smooth out the finer-scale variations of the geomagnetic field. The fold-test is done for both limbs of the fold in the eastern margin of the basin that include Yesilova and Güvendik sites. Remanent Magnetic Susceptibility (RMS) was acquired prior to folding of the Güvendik Syncline (GS, Fig. 1).

3.a. Thermal demagnetization

Thermal demagnetization was performed using a magnetically shielded, laboratory-built furnace. The natural remanent magnetization (NRM) was measured on a 2G Enterprises DC SQUID cryogenic magnetometer. At least seven specimens per site were analysed using progressive stepwise thermal demagnetization at temperature increments of 30 °C or 50 °C, starting from room temperature to the limit of reproducible results.

Demagnetization diagrams (Zijderveld, 1967) through selected data points were used to determine the NRM components (Fig. 3). When the results show a linear decay, usually towards the origin, a magnetization vector is determined. The magnetization vectors were averaged using Fisher (1953) statistics to calculate mean directions per site (Table 1), from which tectonically induced rotations could be determined. As it is still unclear to which stable region the Çankırı Basin formerly belonged, the results are not compared to a pole of a known reference plate, but are instead compared to 0° as a reference direction.

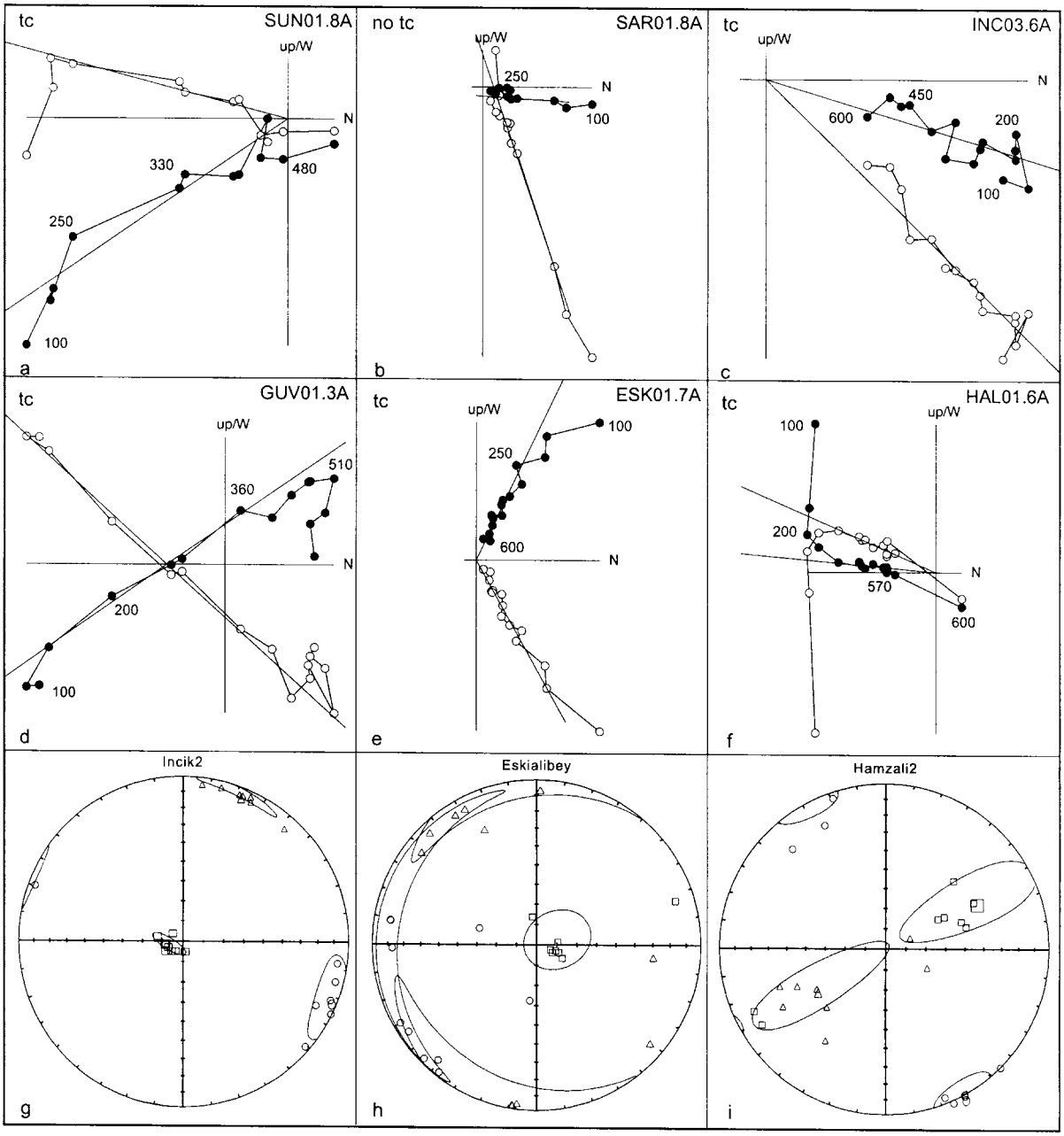

Figure 3. Orthogonal projections of stepwise thermal demagnetization of selected samples from Eocene (a, b) Oligocene (c, d) and Miocene (e, f) sediments. Closed (open) circles represent the projection of the ChRM vector endpoint on the horizontal (vertical) plane. Numbers denote temperatures in °C and tc/no tc indicates after/before bedding plane correction. (g–i) Equal area projection of anisotropy of the magnetic susceptibility with circles/squares/triangles as $k_{min}/k_{max}/k_{int}$ after bedding plane correction.

The palaeolatitudes are plotted in Figure 4 and listed in Table 1.

Apart from a very small and randomly oriented laboratory-induced component removed at 100 °C, a secondary component is sometimes present; it is generally removed between 100 and 200 °C. It has the present-day direction before bedding tilt correction and is thus of Recent origin and a viscous remanence possibly caused by weathering. A characteristic remanent magnetization (ChRM) component is removed at higher temperatures and shows both normal and reversed polarities. Most sites reveal ChRM components demagnetized at temperatures of 570–600 °C (Fig. 3c, e, f) residing in magnetite. Demagnetization at higher temperatures results in randomly directed components. These samples have a relatively high NRM intensity (6–13 mA m^{-1}). Some samples, which are demagnetized at temperatures around 390–420 °C (Fig. 3a), and have relatively low intensities (0.8 mA m^{-1}) have ChRM components which are probably carried by Fe-sulphides. We show an example of a completely overprinted sample with a relatively high intensity (66 mA m^{-1}) and a signal largely destroyed around 250 °C (Fig. 3b). The Oligocene site of Güvendik

Table 1. Results from natural remanent magnetization (NRM) analysis from the sites in the Çankırı Basin

Site	Code	N	D_{notc} (°)	I_{notc} (°)	k	α_{95} (°)	D_{tc} (°)	I_{tc} (°)	k	α_{95} (°)	Rot (°)	Sense ac/c	Age	Palaeolatitude Min	Mean	Max
Sungurlu	SUN	8	153.1	16.4	51.8	7.8	152.9	−12.6	51.8	7.8	27	ac	Eocene	2.4	6.4	10.5
Incik 2	INC2	4	207.3	20.0	187.1	6.7	208.7	−12.5	187.1	6.7	29	c	Eocene	2.9	6.3	9.9
Kalinpelit	KAL	6	357.0	12.5	88.3	7.5	353.5	33.0	88.3	7.2	7	ac	Oligocene	13.6	18.0	22.9
Yesilova	YES	6	53.8	−17.9	83.5	7.4	51.6	22.2	83.5	7.4	52	c	Oligocene	7.5	11.5	15.9
Danaci	DAN	5	347.9	37.6	20.4	17.3	356.3	29.2	20.4	17.3	4	ac	Oligocene	6.0	15.6	27.8
Guvendik	GUV	7	120.9	−45.8	378.8	3.1	144.1	−35.6	378.8	3.1	36	ac	Oligocene	17.7	19.7	21.8
Hamzali 3	HAM3	5	184.8	−44.8	103.9	7.5	178.1	−28.1	103.9	7.5	2	ac	Oligocene	10.6	15.0	19.7
Incik 3	INC3	7	15.6	19.7	35.4	10.3	18.6	44.3	35.4	10.3	19	c	Oligocene	18.6	26.0	35.1
Hamzali 2	HAM2	7	331.7	15.7	72.4	7.1	326.6	14.4	72.4	7.1	33	ac	Oligocene	3.7	7.3	11.1
Kuscali	KUC	7	161.8	−56.2	102.4	6.0	178.5	−59.8	102.4	6.0	2.0	ac	Middle Miocene	34.3	40.7	48.1
Halacli	HAL1	5	198.5	6.1	55.3	10.4	196.9	−21.8	55.3	10.4	17	c	Middle Miocene	5.8	11.3	17.5
Urludag	UR	6	353.1	34.9	58.8	8.8	356.5	43.9	58.8	8.8	4	ac	Late Miocene	19.4	25.7	33.3
Eskialibey	ESK	7	296.9	37.8	60.4	7.8	297.4	39.2	60.4	7.8	62	ac	Late Miocene	17.0	22.2	28.2
Mean																
		2					180.8	−14.1	0.0				Eocene		7.2	
		7					357.4	32.7	8.7	21.6			Oligocene	5.6	17.8	34.8
		2					193.6	−40.9	0.0				Middle Miocene		23.4	
		2					325.8	45.5	0.0				Late Miocene		27	

Corrected (tc) and uncorrected (no tc) for bedding tilt, ages are indicated. N = number of specimens; D, I = site mean ChRM declination and inclination; k = Fisher's precision parameter; $\alpha 95 = 95$ % cone of confidence; Rot = magnitude of rotation; (a)c = (anti)clockwise with a 0° reference direction; min/mean/max concerns palaeolatitude.

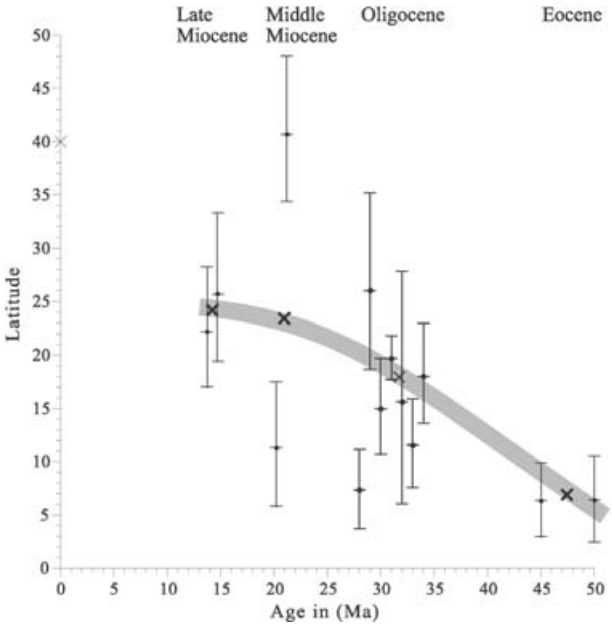

Figure 4. Latitude of the sites from the Çankırı Basin versus time. Crosses and grey zone represent palaeolatitude-means per age (see Table 1).

(Fig. 3d) has two antiparallel components; a reversed component unblocked by 510 °C and a normal component unblocked from 510 °C to 580 °C. We used the reversed component, as it appeared to be most stable.

Only two of the seven Eocene sites show reliable results. One site (Sungurlu), located in the southeast of the Çankırı Basin (Fig. 5), implies an anticlockwise rotation of 27°, while the other site (Incik 2), located in the north indicates a clockwise rotation of 29°. The palaeolatitude of these Eocene sites points to a near-equatorial position (6°). All seven Oligocene sites produced reliable data. The three Oligocene sites located in (south-)west of the Çankırı Basin show no rotation (Danaci and Hamzali 3) to anticlockwise rotations up to 33° (Hamzali 2). In the north, a site with a large clockwise rotation of 19° (Incik 3) and a site with a small anticlockwise rotation of 7° (Kalinpelit) are found. Likewise in the east, a large clockwise rotation of 52° (Yesilova) and a large anticlockwise rotation of 36° (Güvendik) were detected. Although the Oligocene palaeolatitudes are variable, a clear trend is visible, indicating a northward movement of the Çankırı Basin. Two out of three Middle Miocene sites from the south of the Çankırı Basin were found to be reliable, with one site revealing a clockwise rotation (Halaçli) and another site indicating little or no rotation (Kuscali). Of the Late Miocene sites, two out of three are located in the northeast of the basin and imply a further northward movement. One of the late Miocene sites (Ugurludag) shows a small anticlockwise rotation of 4° and another one (Eskialibey) a large anticlockwise rotation of 62°.

3.b. Anisotropy of the magnetic susceptibility

Analysis of the anisotropy of the magnetic susceptibility (AMS) is widely used to establish the sedimentary and tectonic history in weakly deformed sediments. Basically, the AMS of a rock is described by a second-order tensor. This tensor can be visualized by an ellipsoid having three principal axes of maximum, intermediate, and minimum susceptibility (k_{max}, k_{int} and k_{min}, respectively). Here, we characterize the total degree of anisotropy by $P = k_{max}/k_{min}$; the magnetic

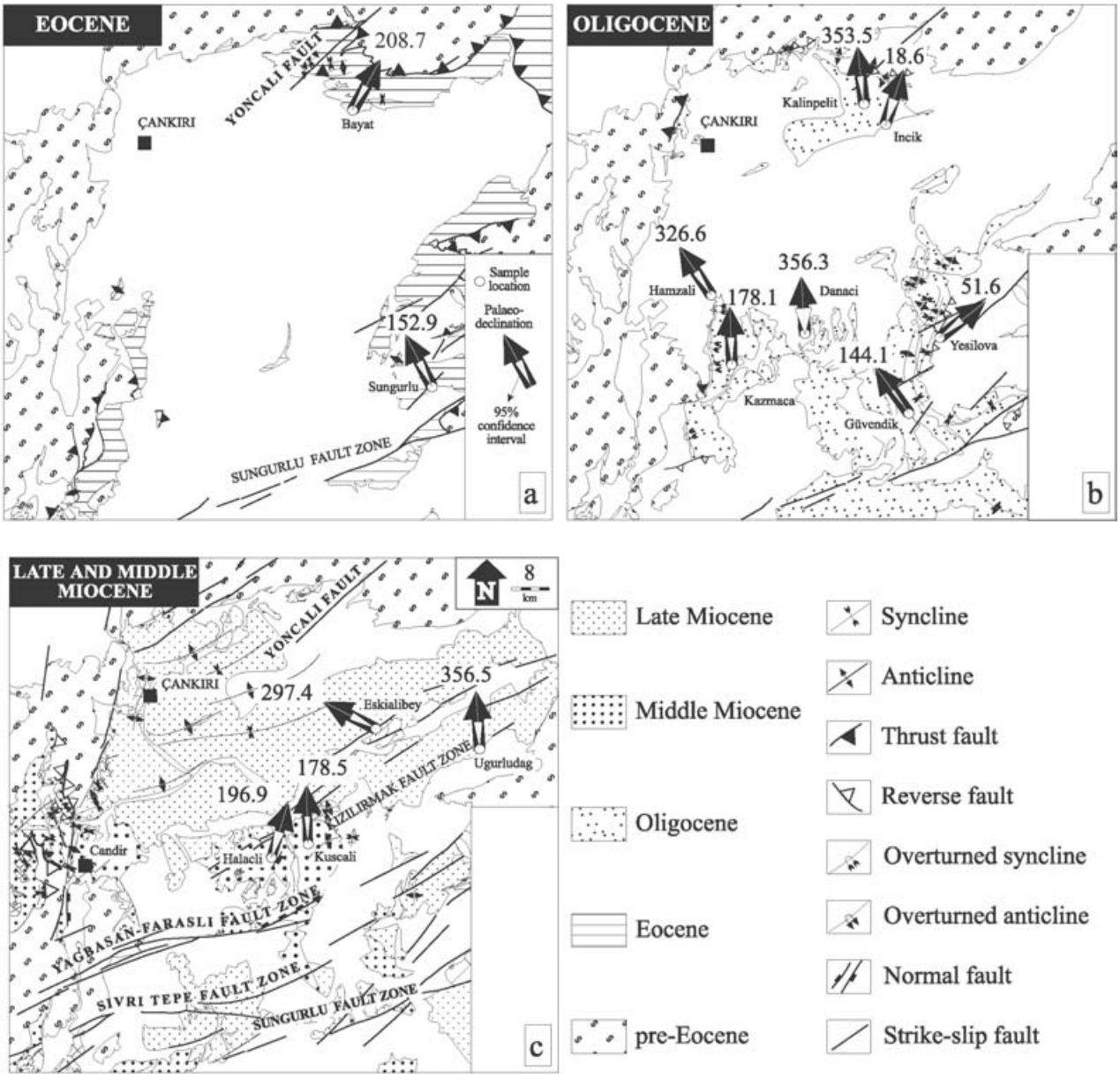

Figure 5. Simplified geological maps and palaeodeclinations of site means with 95 % confidence intervals.

foliation is defined by $F = k_{int}/k_{min}$, while the magnetic lineation is the degree of anisotropy in the magnetic foliation plane and defined by $L = k_{max}/k_{int}$ (see Tarling & Hrouda, 1993). Depositional currents can also account for lineations, but this effect is likely to be minimum in the fine-grained, mostly continental, clays of the Çankırı Basin. In undeformed sediments, the magnetic susceptibility is characterized by an oblate ellipsoid, with the foliation coinciding with the bedding plane. In this case, the magnetic fabric is purely depositional or is related to compactional loading; the k_{min} is perpendicular to the bedding plane and the k_{max} and k_{int} are scattered in the foliation or bedding plane itself. If the rock is strained, this initially results in clustering of k_{max} in the direction of maximum extension or, equivalently, perpendicular to the maximum compression. The k_{min} is still perpendicular to the bedding plane. An increase of the strain causes the ellipsoid to have a more prolate structure. Finally, progressive strain obliterates the prolate ellipsoid into a 'pencil' structure and the depositional fabric becomes overprinted by a tectonic fabric (Tarling & Hrouda, 1993). This pencil cleavage, which can easily be recognized in the field, was not observed in the area of study.

Generally, the AMS results (Table 2) of the sites from the Çankırı Basin show oblate ellipsoids with highly variable mean susceptibilities (53 – 9900 ∞ 10^6 SI) reflecting variable concentrations of magnetic minerals. Error ellipses of the susceptibility axes are calculated according to Jelinek (1978) and are given for k_{max} in Table 2. Seven sites display a

Table 2. Results of anisotropy of magnetic susceptibility (AMS) analysis from the sites in the Çankırı Basin

Name	Code	N	D (°)	I (°)	δD (°)	δI (°)	k_{mean} $*10^{-6}$ SI	F	L	Age (Ma)
Hamzali 1	HAM1	6	347.6	8.6	23.9	5.2	9876.5	1.0094	1.0307	Eocene
Incik 1	INC1	7	141.6	32.3	36.5	10.1	52.8	1.0118	1.0057	Eocene
Kazmaca	KAZ	7	8.9	16.7	7.8	2.2	284.7	1.0314	1.0173	Eocene
Saricalar	SAR	7	89.3	13.9	60.6	8.8	3345.3	1.0522	1.0098	Eocene
Incik 4	INC4	7	182.7	0.4	55.8	12.9	160.6	1.0067	1.0009	Eocene
Sungurlu	SUN	7	52.3	15.4	19.7	10.7	302.7	1.0365	1.0103	Eocene
Incik 2	INC2	6	111	5.8	16.4	9.3	242.1	1.0231	1.0042	Eocene
Kalinpelit	KAL	7	320.9	7.1	37.2	5.7	3783.0	1.0315	1.0064	Oligocene
Yesilova	YES	7	199.6	3.8	50.9	16.5	371.76	1.0314	1.011	Oligocene
Danaci	DAN	7	115.7	13.9	46.1	21.7	327.8	1.0043	1.005	Oligocene
Guvendik	GUV	8	88.5	5.9	17	4.4	242.7	1.0188	1.0085	Oligocene
Hamzali 3	HAM3	7	143	3.3	30	7.4	4795.4	1.0182	1.0067	Oligocene
Incik 3	INC3	8	70.6	2.8	50.8	17.2	684.0	1.0176	1.0047	Oligocene
Hamzali 2	HAM2	7	151.3	0.0	12	9.7	6653.1	1.0145	1.0105	Oligocene
Sulakyurt	SUL	7	255.3	1.8	34.7	8.4	121.85	1.0193	1.0026	Late Miocene
Urludag	UR	7	52	3.2	26.5	16.6	207.5	1.0273	1.005	Late Miocene
Eskialibey	ESK	8	280	9.8	67.9	7	259.6	1.0297	1.0032	Late Miocene
Kuscali	KUC	6	342.6	2.1	39.2	15.8	1052.3	1.0199	1.0045	Middle Miocene
Halacli	HAL1	7	311.6	4.2	53.7	14	1105.2	1.0354	1.0032	Middle Miocene
Mahmatlar	MAH	7	43.8	5.7	8.9	5.4	1856.7	1.0102	1.0183	Middle Miocene

Corrected for bedding tilt, ages are indicated. N = number of specimens; D, I = mean azimuth and dip of k_{max} axes; δD, δI = errors on mean k_{max} axes; F = magnetic foliation (k_{int}/k_{min}); L = magnetic lineation (k_{max}/k_{int}).

well-defined clustering of the k_{max}-axes, indicating the extension direction or, equivalently, the compression perpendicular to it. Three Eocene sites (Kazmaca, Sungurlu, Incik 2; Fig. 6) identify a (N)NE–(S)SW direction of the k_{max}-axes and one Eocene site (Hamzali 1) indicates a NNW–SSE direction of the k_{max}-axes. Directions are shown before and after correction for rotation in Figure 6. The Oligocene site at Güvendik reveals a clear clustering of the k_{max}-axes along an E–W direction, while the Kalinpelit site implies roughly a NW–SE direction. The k_{int} and k_{min}-axes of Hamzali 2 girdle around the k_{max}-axes, indicating deformation. Finally, the Late Miocene site of Sulakyurt exhibits a ENE–WSW direction of the k_{max}-axes. The remaining sites show a large scatter in k_{max}-axes and are not interpreted.

4. Discussion

4.a. Palaeostress

By using multi-source data including satellite and aerial-photo remote sensing, seismic interpretation, palaeostress inversion, and tectono-stratigraphic studies in the Çankırı Basin. Kaymakci, White & Van Dijk (2000, 2003) have documented that this basin has evolved in at least four different phases of tectonic deformation. The first phase is characterized by thrusting with approximately NW–SE-oriented σ_1 and is most likely to be of Late Cretaceous to Paleocene age. The second phase is of Late Paleocene to Early Miocene age and is characterized by two different stress configurations, one related to the basement and the other to the basin infill and the surrounding rim. The rim and the basin infill have a near-radial σ_1 and sub-vertical σ_3 pattern associated with thrusting, while the basement is characterized by a NNE–SSW-oriented σ_1 and sub-vertical σ_2, indicating coeval strike-slip deformation. The third phase exhibits an overall extensional deformation with concentric σ_3 and sub-vertical σ_1 pattern in the Early to Middle Miocene interval. The fourth phase is characterized by a NW–SE-oriented σ_1 and sub-vertical σ_2. This is explained in terms of regional transcurrent tectonics from the Late Miocene to present (for details of palaeostress information, refer to Kaymakci, White & Van Dijk, 1998, and Kaymakci, 2000).

4.b. Back-rotations

The main structural trends of the Çankırı Basin were back-rotated, according to the amounts of nearby palaeodeclination. In Figure 7, back-rotation of the Güvendik Syncline is illustrated. After back-rotation of different segments of the Güvendik Syncline and the Karacay Reverse Fault, it was observed that the curved syncline becomes a NW–SE-trending straight fold. A similar procedure was followed to restore the other main structural trends in the northern and western parts of the Çankırı Basin.

Orientations of the AMS results for the Eocene become parallel to one of the stress trajectories (σ_2 in the north and $\sigma 3$ trajectories in the southeast, Fig. 6). This relationship may indicate that in Eocene times pure shear conditions were the main deformation process while in the Oligocene simple shear was dominant. Larger rotations in the Oligocene than in the Eocene may support this interpretation. More data are needed to validate and confirm this argument.

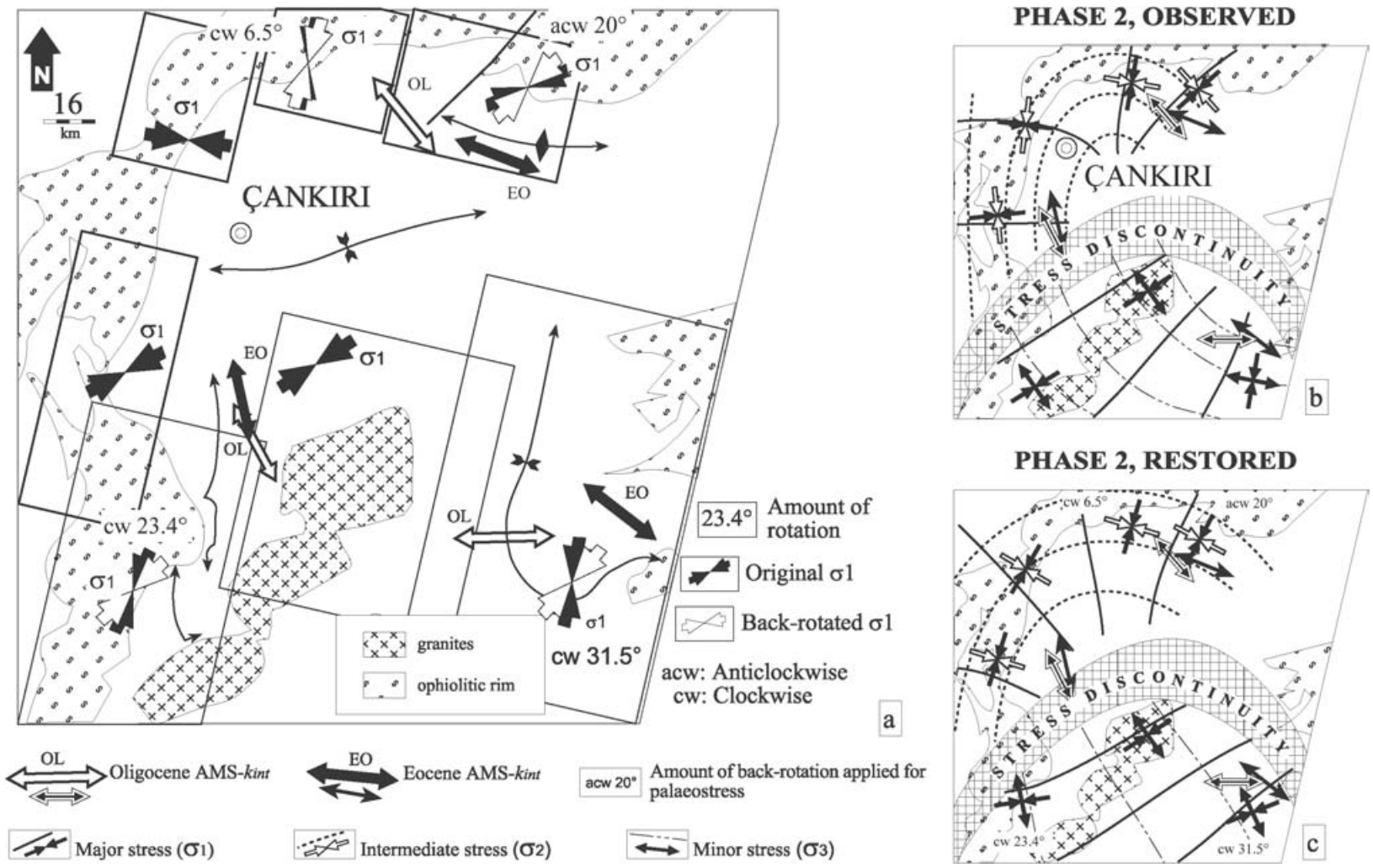

Figure 6. (a) Outline map indicating k_{int} orientations, adjacent to major fold axial trends and palaeostress orientations for each time interval. Boxes are sub-areas which are used to generalize mean stress orientations (see Kaymakci, 2000, and Kaymakci, White & Van Dijk, 2000). (b, c) observed and restored/back-rotated (according to palaeodeclination data) palaeostress trajectories and AMS results. Note that only the stress orientations for phase 2 (Late Paleocene to Early Miocene) are back-rotated. No major rotations were observed after Middle Miocene, therefore deformation phases 3 and 4 are not back-rotated.

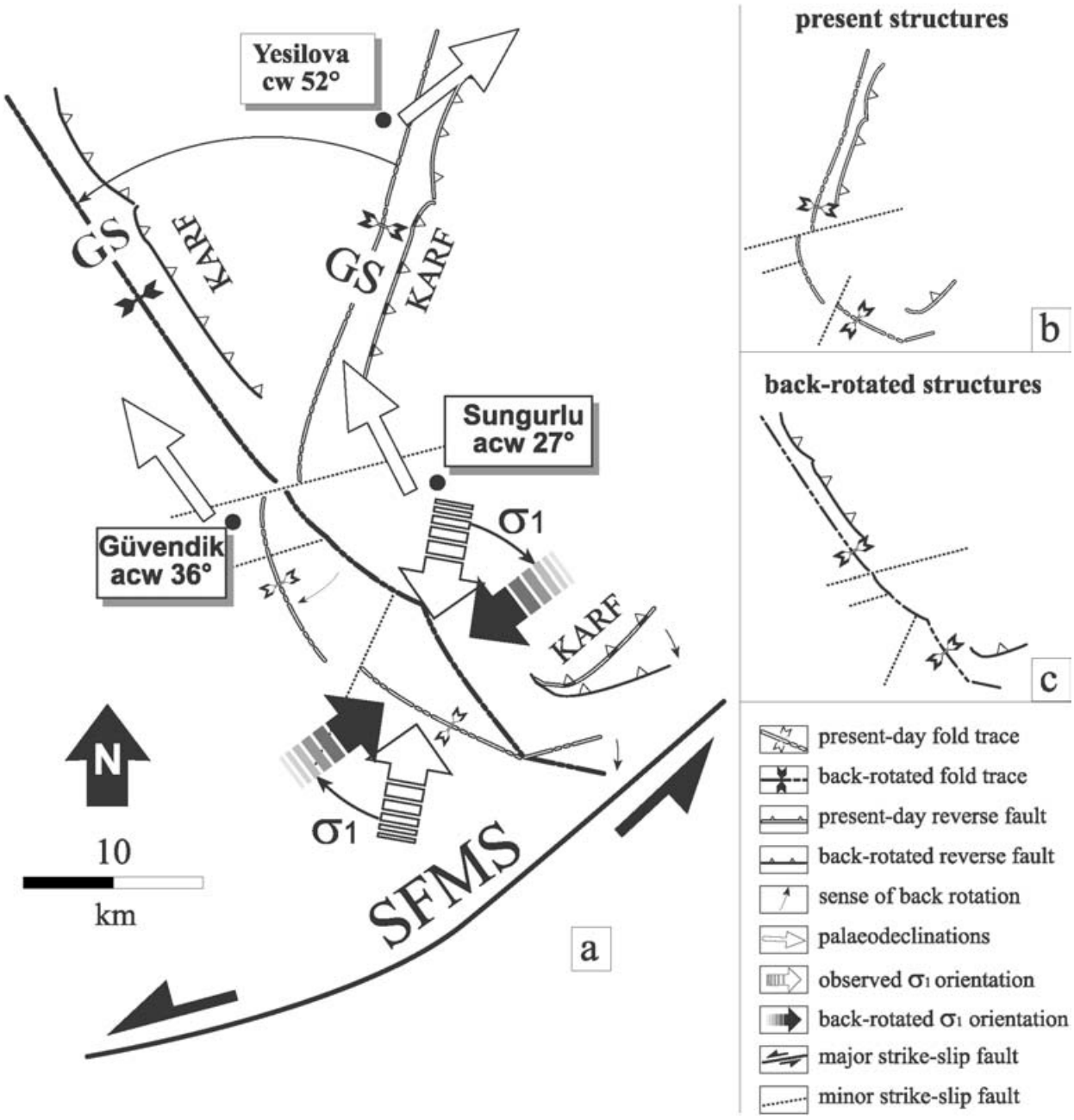

Figure 7. (a) Back-rotation of Güvendik Syncline (GS) and Karaçay Reverse Fault (KARF) using palaeodeclination results in the Eastern margin of the Çankırı Basin. Note σ_1 orientations become orthogonal to the GS and KARF after back-rotation. (b, c) Present-day and back-rotated structures are illustrated separately. acw – anticlockwise; cw – clockwise; SFMS – Master Strand of the Sungurlu Fault.

4.c. Interpretations

This study has provided the first palaeomagnetic results relevant to the evolution of the Çankırı Basin. In general, the results show predominantly anticlockwise rotations in the western margin of the basin and clockwise rotations in the east during Eocene and Oligocene times. Furthermore, the data seem to indicate no rotation of the Kırşehir Block since the Oligocene. Magnetic inclinations of most sites indicate a northwards drift of the region from the Eocene to Middle Miocene. Our palaeomagnetic data concern Eocene and younger rocks and therefore are in accordance with the latest three of the four deformation phases; these are: phase 2 (Late Paleocene to Early Miocene), phase 3 (late-Early to Middle Miocene) and phase 4 (Late Miocene to present). In the western margin the samples from the older parts of the Oligocene units (Hamzali-2) show more rotation than the younger samples (Hamzali-3). This may indicate syn-depositional deformation within the basin. In addition, the Oligocene units (Incik Formation)

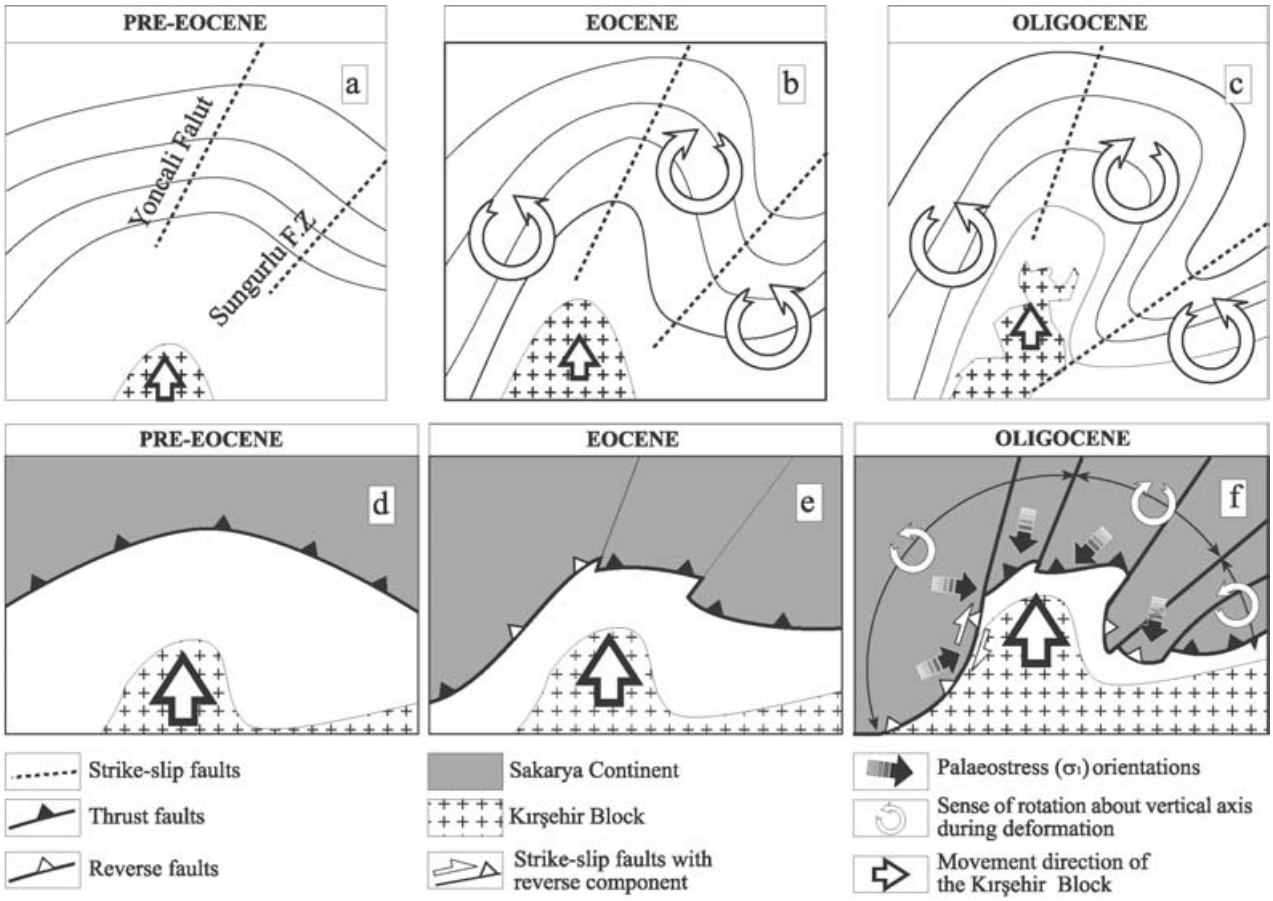

Figure 8. (a–c) Back-rotation of structural trends of the Çankırı Basin. (d–f) Palinspastic reconstructions based on back-rotations of palaeodeclinations. Note stress (σ_1) orientations and pre-Eocene curved outline of the Çankırı Basin after back-rotation of its margins.

comprise a number of syn-depositional progressive unconformities indicative of coupling of deposition and deformation (see also Kaymakci, 2000).

The Eocene and Oligocene anticlockwise rotation in the western rim and the clockwise rotation in the northeastern rim together with the northward drift of the basin can be explained by an indentation model. The Kırşehir Block is the indentor while the Sakarya Continent (see Fig. 1a) is the indented block. Due to the irregular nature of the Kırşehir Block in its northern tip (represented by granitoids in the southern side of the Çankırı Basin), intense deformation resulted within the Sakarya Continent and in the infill of the Çankırı Basin (represented by combined thrusting and strike-slip faulting, Fig. 8), which resulted in the rotation of rims of the Çankırı Basin away from the zone of intense strain. This relation is also reflected in the palaeostress orientations showing a radial σ_1 pattern of thrusting in the northern part of the Çankırı Basin and a strike-slip pattern in the sides of the indentor (western and eastern margins of the Çankırı Basin). This is also described from sandbox model experiments (Zweigel, 1998) and has been modelled by Tapponier *et al*. (1982) and Marshak (1988).

In addition, after the main structural trends of the Çankırı Basin are back-rotated successively for the Oligocene and Eocene (Fig. 8), the structural trends are still curved (northwards convex) for the pre-Eocene period. Considering that the southern margin of the Sakarya Continent was straight prior to indentation of the Kırşehir Block, the resultant (left over) curved pattern of the Sakarya Continent (Fig. 8) may indicate that the indentation process pre-dates Eocene times. In the course of the indentation process, a radial pattern of σ_1 in the basin infill and the rim is expected and indeed found (compare σ_1 orientations in Fig. 6b, c). Furthermore, the suture zone between the colliding blocks divides the region into two different tectonic regimes (stress discontinuity in Fig. 6b, c) where thrusting in the Sakarya Continent and coeval strike-slip deformation in the Kırşehir Block are recognized (see also Kaymakci, White & Van Dijk, 2003). The palaeomagnetic results of the Çankırı Basin, from the Middle and (except Eskialibey) Late Miocene yielded no rotation, possibly implying the end of the indentation process. This is in agreement with the palaeostress and stratigraphic results discussed in Kaymakci (2000) and Kaymakci, White & Van Dijk (2000, 2003).

Finally, the trends of the k_{max} orientations, the adjacent major structural trends and the constructed palaeostress orientations (see Kaymakci, White & Van Dijk, 2000, 2003) are all in good agreement and

validate the proposed tectonic evolution of the Çankırı Basin (Fig. 6). The indentation process is the main mechanism for the rotation of the rim of the Çankırı Basin which resulted in its Ω-shaped outline.

5. Conclusions

(1) The palaeomagnetic results from the Eocene to Oligocene sediments of the Çankırı Basin show that the western and southeastern margins of the Çankırı Basin underwent anticlockwise rotations and clockwise rotations in the east while no rotation has taken place for the Kırşehir Block at least since Oligocene times.
(2) In the Middle and Late Miocene no rotation took place except at one of the Late Miocene sites (Eskialibey) in the northeastern part of the Çankırı Basin, implying that all major rotations took place prior to Middle Miocene times. Hence, the Early Tertiary compressional period, and therefore the indentation process, ended before Middle Miocene times.
(3) The Çankırı Basin has undergone northward drift since Eocene times, as indicated by inclination data. These results, together with rotation of margins of the Çankırı Basin, are in good agreement with the proposed indentation model for the Kırşehir Block. The palaeostress data and AMS orientations support the proposed evolutionary history of the Çankırı Basin and hence development of curved orogenic belts due to indentation.

Acknowledgements. Authors of this paper would like to thank Hans de Bruijn, Albert van Meulen, Engin Unay and Gerçek Saraç for detailed micro-mammal (rodent) ages and their help during the field studies. Cemil Arli is thanked for his help in transportation of the samples. This study is supported by Kocaeli University, Turkey YLS-grant.

References

BARKA, A. A. 1992. The North Anatolian fault zone. *Annales Tectonicae* **VI** supp., 164–95.

BARKA, A. A. & HANCOCK, P. L. 1984. Neotectonic deformation patterns in the convex-northwards arc of the North Anatolian Fault Zone. In *The geological evolution of the Eastern Mediterranean* (eds J. E. Dixon and A. H. F. Robertson), pp. 763–74. Geological Society of London, Special Publication no. 17.

CHANNELL, J. E. T., TÜYSÜZ, O., BEKTAS, O. & ŞENGÖR, A. M. C. 1996. Jurassic–Cretaceous paleomagnetism and paleogeography of the Pontides (Turkey). *Tectonics* **15**(1), 201–12.

DECOURT, J., RICOU, L. E. & VRIELYNCK, B. 1993. *Atlas Tethys, Paleoenvironmental maps*. Beicip-Franlab.

EVANS, I. & HALL, S. A. 1990. Paleomagnetic constraints on the tectonic evolution of the Sakarya Continent, northwestern Anatolia. *Tectonophysics* **182**, 357–72.

FISHER, R. A. 1953. Dispersion on a sphere. *Proceedings of the Royal Society London* **217**, 295–305.

GÖRÜR, N., OKTAY, F. Y., SEYMEN, I. & ŞENGÖR, A. M. C. 1984. Palaeotectonic evolution of the Tuzgölü basin complex, Central Turkey: Sedimentary record of a neotethyan closure. In *The geological evolution of the Eastern Mediterranean* (eds J. E. Dixon and A. H. F. Robertson), pp. 467–82. Geological Society of London, Special Publication no. 17.

GÜRSOY, H., PIPER, J. D. A., TATAR, O. & TEMIZ, H. A. 1997. Paleomagnetic study of the Sivas Basin, central Turkey: crustal deformation during lateral extrusion of the Anatolian Block. *Tectonophysics* **271**, 89–105.

JELINEK, V. 1978. Statistical processing of anisotropy of magnetic susceptibility on groups of specimens. *Studia Geophysica et Geodaetica* **22**, 50–62.

KAYMAKCI, N. 2000. *Tectono-stratigraphical evolution of the Çankırı Basin (Central Anatolia, Turkey)*. Ph.D. Thesis, Utrecht University, The Netherlands. Geologica Ultraiectina, no. 190, 248 pp.

KAYMAKCI, N. & KOÇYIĞIT, A. 1995. Mechanism and basin generation in the splay fault zone of the North Anatolian Fault Zone. *E. U. G. 8th Conference on the Earth Sciences, Strasbourg* (abstract).

KAYMAKCI, N., WHITE, S. H. & VAN DIJK, P. M. 1998. Paleostress inversion in a multi-phase deformed area: Çankırı Basin (central Anatolia). *3rd International Turkish Geology. Symposium: Progress in understanding the Geology of* Turkey. 31 August–4 Sept. (1998) METU, Ankara, Turkey (abstract).

KAYMAKCI, N., WHITE, S. H. & VAN DIJK P. M. 2000. Paleostress inversion in a multi-phase deformed area: Kinematic and structural evolution of the Çankırı Basin (central Turkey): Part 1. In *Tectonics and Magmatism in Turkey and its Surroundings* (eds E. Bozkurt, J. A. Winchester and J. Piper), pp. 445–73. Geological Society of London, Special Publication no. 173.

KAYMAKCI, N., WHITE, S. H. & VAN DIJK, P. M. 2003. Kinematic and structural development of the Çankırı Basin (Central Anatolia, Turkey): A paleostress inversion study. *Tectonophysics* (in press).

KETIN, I. 1966. Tectonic units of Anatolia (Asia Minor). *Maden Tetkik ve Arama Enstitüsü. Dergisi* **66**, 23–34.

KOÇYIĞIT, A. 1991. An example of an accretionary forearc basin from north Central Anatolia and its implications for the history of subduction of Neotethys in Turkey. *Geological Society of America Bulletin* **103**, 22–36.

KOÇYIĞIT, A., ÖZKAN, S. & ROJAY, B. F. 1988. Examples from the fore-arc basin remnants at the active margin of northern Neotethys; Development and emplacement age of the Anatolian Nappe, Turkey. *Middle East Technical University Journal of Pure and Applied Sciences* **21**(1–3), 183–210.

MARSHAK, S. 1988. Kinematics of orocline and arc formation in thin-skinned orogens. *Tectonics* **7**, 73–88.

MICHEL, G. W., WALDHÖR, M., NEUGEBAUER, J. & APPEL, E. 1995. Sequential rotation of stretching axes and block rotations: a structural and paleomagnetic study along the North Anatolian Fault. *Tectonophysics* **243**, 97–118.

MORRIS, A. & ROBERTSON, A. H. F. 1993. Miocene remagnetisation of carbonate platform and Antalya Complex units within the Isparta Angle, SW Turkey. *Tectonophysics* **220**, 243–66.

OKAY, A. I., HARRIS, N. B. W. & KELLEY, S. P. 1998. Exhumation of blueschists along a Tethyan suture in northwest Turkey. *Tectonophysics* **284**, 275–99.

ORAL, M. B., REILINGER, R. E., TOKSOZ, M. N., KING, R. W., BARKA, A. A., KINIK, I. & LENK, O. 1997. Global positioning system offers evidence of plate motions in Eastern Mediterranean. *EOS, Transactions American Geophysical Union* **76**(2), 9–11.

PIPER, J. D. A., MOORE, J., TATAR, O., GÜRSOY, H. & PARK, R. G. 1996. Paleomagnetic study of crustal deformation across an intracontinental transform: the North Anatolian Fault Zone in Northern Turkey. In *Paleomagnetism of the Eastern Mediterranean Regions* (eds A. Morris and D. H. Tarling), pp. 299–310. Geological Society of London, Special Publication no. 105.

PIPER, J. D. A., TATAR, O. & GÜRSOY, H. 1997. Deformational behaviour of continental lithosphere deduced from block rotations across the North Anatolian fault zone in Turkey. *Earth and Planetary Science Letters* **150**, 191–203.

PLATZMAN, E. S., PLATT, J. P., TAPIRDAMAZ, C., SANVER, M. & BUNDLE, C. C. 1994. Why are there no clockwise rotations along the North Anatolian Fault? *Journal of Geophysical Research* **99**, 21705–16.

PLATZMAN, E. S., TAPIRDAMAZ, C. & SANVER, M. 1998. Neogene anticlockwise rotation of central Anatolia (Turkey): Preliminary paleomagnetic and geochronological results. *Tectonophysics* **299**, 175–89.

ROBERTSON, A. H. F. & DIXON, J. E. 1984. Introduction: aspects of the geological evolution of the Eastern Mediterranean In *The Geological Evolution of the Eastern Mediterranean* (eds J. E. Dixon and A. H. F. Robertson), pp. 1–74. Geological Society of London, Special Publication no. 17.

ROBERTSON, A. H. F., DIXON, J. E., BROWN, S., COLLINS, A., MORRIS, A., PICKETT, E., SHARP, I. & USTAOMER, T. 1996. Alternative tectonic models for the Late Paleozoic–Early Tertiary development of the Tethys in the Eastern Mediterranean region. In *Paleomagnetism of the Eastern Mediterranean Regions* (eds A. Morris and D. H. Tarling), pp. 239–63. Geological Society of London, Special Publication no. 105.

ROJAY, B. F. 1995. Post-Triassic evolution of central Pontides: Evidence from Amasya region, Northern Anatolia. *Geologica Romana* **31**, 329–50.

SANVER, M. & PONAT, E. 1981. Kırşehir ve dolaylarina iliskin paleomagnetik bulgular. Kırşehir Masifinin rotasyonu. *Istanbul Yerbilimleri* **2**, 2–8.

SARIBUDAK, M., SANVER, M. SENGOR, A. M. C. & GÖRÜR, N. 1990. Paleomagnetic evidence for substantial rotation of the Elmacik flake within the North Anatolian Fault Zone, NW Turkey. *Geophysical Journal International* **102**, 563–8.

ŞENGÖR, A. M. C., ŞAROĞLU, F. & GÖRÜR, N. 1985. Strike-slip deformation and related basin formation in zones of tectonic escape: Turkey as a case study. In *Strike-Slip Deformation Basin Formation and Sedimentation* (eds K. T. Biddle and N. Christie-Blick), pp. 227–64. Society of Economic Palaeontologists and Mineralogists, Special Publication no. 37.

ŞENGÖR, A. M. C. & YILMAZ, Y. 1981. Tethyan evolution of Turkey: a plate tectonic approach. *Tectonophysics* **75**, 181–241.

ŞENGÖR, A. M. C., YILMAZ, Y. & SUNGURLU, O. 1984. Tectonics of the Mediterranean Cimmerides: nature and evolution of the western termination of palaeo-Tethys. In *The Geological Evolution of the Eastern Mediterranean* (eds J. E. Dixon and A. H. F. Robertson), pp. 77–112. Geological Society of London, Special Publication no. 17.

TAPPONIER, P., PELTZER, G., LE DAIN, A. Y., ARMIJO, R. & COBBOLD, P. 1982. Propagating extrusion tectonics in Asia: new insights from simple experiments with plasticine. *Geology* **10**, 611–16.

TARLING, D. H. & HROUDA, F. 1993. *The magnetic anisotropy of rocks*. London: Chapman and Hall, 217 pp.

TATAR, O., PIPER, J. D. A., PARK, R. G. & GÜRSOY, H. 1995. Paleomagnetic study of block rotations in the Niksar overlap region of the North Anatolian Fault Zone, Central Turkey. *Tectonophysics* **244**, 251– 66.

TOPRAK, V., SAVASÇIN, Y., GÜLEÇ, N. & TANKUT, A. 1996. Structure of the Galatean Volcanic Province, Turkey. *International Geology Review* **38**, 747–58.

TÜYSÜZ, O. 1993. Karadenizden Orta Anadolu'ya bir jeotravers. *Türkiye Petrol Jeologlari Bülteni* **5**(1), 1–33.

TÜYSÜZ, O., DELLALOĞLU, A. A. & TERZIOĞLU, N. 1995. A magmatic belt within the Neo-Tethyan suture zone and its role in the tectonic evolution of northern Turkey. *Tectonophysics* **243**, 173–91.

VAN DER VOO, R. 1968. Paleomagnetism and the Alpine tectonics of Eurasia, part 4. Jurassic, Cretaceous and Eocene pole positions from NE Turkey. *Tectonophysics* **6**, 251–69.

ZIJDERVELD, J. D. A. 1967. Demagnetisation of rock: analysis of results. In *Methods in paleomagnetism* (eds D. W. Collinson, K. M. Creer and S. K. Runcorn), pp. 254–86. Amsterdam: Elsevier.

ZWEIGEL, P. 1998. Arcuate accretionary wedge formation at convex plate margin corners: results of sandbox analogue experiments. *Journal of Structural Geology* **20**, 1597–609.